Thermochimica Acta 512 (2011) 240–246

Contents lists available at ScienceDirect

Thermochimica Acta

journal homepage: www.elsevier.com/locate/tca

Thermodynamic description of the Au–Ag–Ge ternary system

J. Wang[a,d,*], Y.J. Liu[b], C.Y. Tang[a], L.B. Liu[c], H.Y. Zhou[a], Z.P. Jin[c]

[a] School of Materials Science and Engineering, Guilin University of Electronic Technology, Guilin, Guangxi 541004, PR China
[b] Western Transportation Institute, Montana State University, Bozeman, MT 59715, USA
[c] School of Materials Science and Engineering, Central South University, Changsha, Hunan 410083, PR China
[d] Swiss Federal Laboratories for Materials Science and Technology, Laboratory for Joining and Interface Technology, Überlandstrasse 129, Dübendorf, Zürich CH-8600, Switzerland

ARTICLE INFO

Article history:
Received 23 August 2010
Received in revised form 27 October 2010
Accepted 2 November 2010
Available online 11 November 2010

Keywords:
Au–Ge-based alloys
Phase diagram
Thermodynamics
CALPHAD
Au–Ag–Ge ternary system

ABSTRACT

The Ag–Ge binary system has been assessed thermodynamically using the CALPHAD method through the Thermo-calc® software based on the available experimental information from the published literature. The solution phases including liquid, fcc_A1(Au,Ag), and diamond_A4(Ge), were modeled as substitutional solutions and their excess Gibbs energies were expressed by the Redlich–Kister polynomial. On the basis of the previous assessments of the Au–Ag and Au–Ge binary systems, the thermodynamic description of the Au–Ag–Ge ternary system has been performed. The liquidus projection and several vertical sections of this ternary system have been calculated, which are in good agreement with the reported experimental data.

1. Introduction

High-Pb containing solders (e.g. Pb–5 wt.% Sn) as high-temperature solders have been widely used in electronic packaging industries. However, Pb is harmful to both the environment and human health. The development of high-temperature Pb-free solders to replace the conventional high-Pb containing solders has become an important issue now [1–3]. Despite the high price, Au-based alloys such as Au–Sn, Au–Sb, Au–Si and Au–Ge eutectic alloys are useful for bonding applications [4–11]. Especially, Au–20 wt.% Sn eutectic alloy has been used widely in high power electronic and optoelectronic devices because it has superior resistance to corrosion and high electrical and thermal conductivity as well as high mechanical strength [3–9]. Recently, Au–Ge-based alloys are attractive as a great potential candidate for high temperature Pb-free solders in the electronic and optoelectronic packaging [10,11]. However, to reduce the costs of Au-based solders, the alloying elements including Ag, Al, Bi, Cu, Ga, Ge, In, Sb, Zn, etc. may be added to replace a part of the Au. In order to understand better the role of alloying elements and to develop new Au-based solders, knowledge of the precise phase diagrams and reliable thermodynamic properties of the Au-based alloys is indispensable. Recently, thermodynamic descriptions of many binary and ternary systems such as Au–Pb, Au–Al, Au–In, Au–Zn binary systems and Au–Ag–Si, Au–Ag–Sn, Au–Bi–Sb, Au–Ge–Sn, Au–Ge–Sb, Au–Ge–Si, Au–Ag–Pb, Au–Sb–Si, Au–In–Sn, Au–In–Sb, Au–Si–Sn and Au–Co–Sn ternary systems have been developed by Wang, Liu and Jin [12–27] using the CALPHAD method [28,29]. As an essential contribution to establish a consistent and available thermodynamic database of the multicomponent Au-based alloys, the purpose of the present work was to obtain a thermodynamic description of the Au–Ag–Ge ternary system.

Among the three binary sub-systems, the Au–Ag and Au–Ge binary systems have been well assessed thermodynamically by Hassam et al. [30] and Wang et al. [16], respectively. The calculated phase diagrams of the Au–Ag and Au–Ge binary systems are shown in Figs. 1 and 2, respectively. Thermodynamic parameters for the Gibbs energies of various phases in the Au–Ag and Au–Ge binary systems obtained by Hassam et al. [30] and Wang et al. [16] were employed directly in the present optimization and calculation. The Ag–Ge binary system was reviewed previously by Olesinski and Abbaschian [31] and was optimized by Chevalier [32], which can reproduce most experimental information on thermodynamic properties and phase boundaries. However, the lattice stabilities of the elements Ag and Ge used in Ref. [32] are different from those proposed recently by Dinsdale [33]. In order to achieve the compatibility of thermodynamic databases in the multi-component systems, thermodynamic parameters of various phases in the Ag–Ge binary system were reassessed firstly in the present work. Then, based on the already optimized Au–Ag

* Corresponding author at: Swiss Federal Laboratories for Materials Science and Technology, Laboratory for Joining and Interface Technology, Überlandstrasse 129, Dübendorf, Zürich CH-8600, Switzerland. Tel.: +41 44 823 4250.
E-mail addresses: wangjiang158@gmail.com, jiang.wang@empa.ch (J. Wang).

0040-6031/$ – see front matter © 2010 Elsevier B.V. All rights reserved.
doi:10.1016/j.tca.2010.11.003

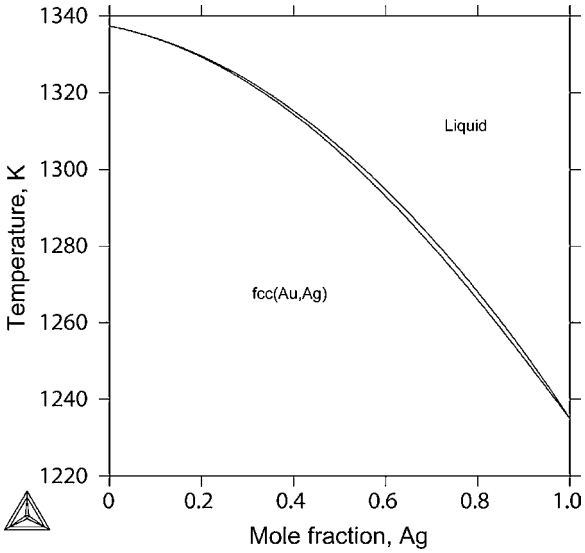

Fig. 1. Calculated phase diagram of the Ag–Au binary system by Hassam et al. [30].

and Au–Ge binary systems, the Au–Ag–Ge ternary system was optimized further using the CALPHAD method [28,29] through Thermo-calc® software [34]. Finally, thermodynamic parameters describing various phases in this ternary system were obtained.

2. Experimental information

2.1. The Ag–Ge binary system

In the Ag–Ge binary system, there are three condensed phases including liquid, fcc_A1(Ag) and diamond_A4(Ge), which form a eutectic reaction. Using thermal analysis, Briggs et al. [35], Maucher [36], Hume-Rothery et al. [37], Predel and Bamlstahl [38] and Hassam et al. [39] determined the temperature and composition of this eutectic reaction as given in Table 1. The experimental data [35–39] on this eutectic reaction are in good agreement with each other and were accepted in the present work.

Phase boundaries of the liquid phase were measured by Briggs et al. [35] and Maucher [36] by means of thermal analysis in the whole composition range. Predel and Bamlstahl [38] determined

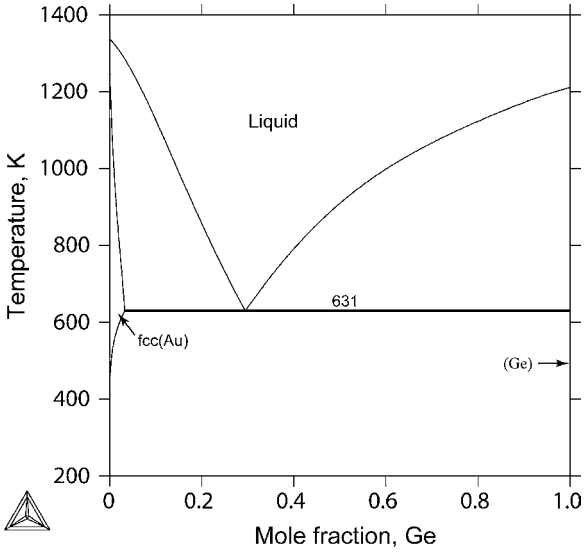

Fig. 2. Calculated phase diagram of the Au–Ge binary system by Wang et al. [16].

Table 1
Eutectic reaction in the Ag–Ge binary system.

Reaction	T (K)	Composition (x^{L}_{Ge})	Reference
L ↔ fcc_A1(Ag) + diamond_A4(Ge)	923	0.260	[35]
	922	0241	[36]
	924	–	[37]
	923	0.240	[38]
	923.5	0.240	[39]
	923.4	0.249	[32]
	921	0.249	This work

the liquidus in the composition range from 64 at.% Ag to 82 at.% Ag using thermal analysis. The experimental results in Refs. [35,36,38] are generally consistent with each other and were used in the present optimization.

The solubility of Ge in the fcc_A1(Ag) phase below the eutectic temperature was determined by Owen and Rowlands [40] through lattice parameter measurements using X-ray powder method. Pollock [41] reported the composition of the fcc_A1(Ag) phase at room temperature (about 300 K) from thermoelectric measurements. The experimental information on the solubility of Ag in diamond_A4(Ge) could not be found in the literature. Therefore, the solubility of Ge in fcc_A1(Ag) was taken into account, while the solubility of Ag in diamond_A4(Ge) was neglected in the present optimization.

The enthalpies of mixing of liquid Ag–Ge alloys referred to liquid Ag and liquid Ge were measured by Catanet et al. [42,43] at 1280 K using calorimetry method. Batalin et al. [44] determined the enthalpies of mixing of liquid Ag–Ge alloys at 1430 K by means of the electromotive force (EMF) method. The experimental results obtained by Castanet et al. [42,43] show good agreement and are also compatible with the experimental data of Batalin et al. [44], although their experimental values are slightly discrepant due to the different measured temperatures. It should be noticed that the enthalpies of mixing determined by Batalin et al. [44] are deduced from the EMF measurements. The enthalpies of mixing measured directly by Catanet et al. [42,43] through the calorimetric experiments are much more reliable and were thus given larger weights than the data of Batalin et al. [44] in the present optimization.

Activities of Ag in the liquid Ag–Ge alloys were determined by Batalin et al. [44] at 1430 K using the EMF method, by Eremenko et al. [45] at 1378 K through the vapour measurements and by Martin-Garin et al. [46] at 1250 K and Oktay [47] at 1416 K using the Knudsen mass spectrometry technique. The activities of Ag determined by Batalin et al. [44], and Martin-Garin et al. [46] are in good agreement and are also consistent with the experimental values of Eremenko et al. [45] in the Ag-rich part, although their experimental temperatures are different. However, the experimental data of Batalin et al. [44], Eremenko et al. [45] and Martin-Garin et al. [46] differ considerably from the scattered experimental data reported by Oktay [47], especially in the Ag-rich part. On the other hand, Eremenko et al. [45] and Martin-Garin et al. [46] determined the activities of Ge in the liquid Ag–Ge alloys at 1250 K and 1378 K, respectively. The activities of Ge determined by Eremenko et al. [45] and Martin-Garin et al. [46] show good agreement. Considering the accordance of most experimental data, the measured values in Refs. [44–46] were taken into account, while the reported data by Oktay [47] at 1416 K are scattered and thus were given up in the present optimization.

2.2. The Au–Ag–Ge ternary system

The thermodynamic properties and phase relations of the Au–Ag–Ge ternary system were investigated experimentally by several authors [39,48–51]. Prince et al. [52] and Borzone et al. [53] reviewed this ternary system when compiled phase diagrams of

Au-based alloys. According to the experimental results in Ref. [39], no stable ternary compound was found in the Au–Ag–Ge ternary system.

The thermodynamic properties of liquid alloys in the Au–Ag–Ge ternary system were investigated by the different researchers [48–51]. Hassam and Gaune-Escard [48] as well as Hassam et al. [49] measured the enthalpies of mixing of the liquid Au–Ag–Ge ternary alloys at 1373 K along the different sections – x_{Ag}:x_{Ge} = 1:3, x_{Ag}:x_{Ge} = 1:1, x_{Ag}:x_{Ge} = 3:1 and x_{Au}:x_{Ge} = 1:3, x_{Au}:x_{Ge} = 1:1, x_{Au}:x_{Ge} = 3:1 by the direct reaction calorimetry. At the same time, Castanet [50] reported the enthalpies of formation of the liquid Au–Ag–Ge ternary alloys at 1348 K. The experimental values measured by Hassam and Gaune-Escard [48], Hassam et al. [49] and Castanet [50] are in reasonable agreement with each other, although there is a small temperature difference (25 K) in their experiments. In addition, the activities of Ag in the ternary liquid Au–Ag–Ge alloys at 1416 K were investigated by Yu and Howard [51] using the Knudsen cell-mass spectrometer method. However, the experimental values for the activities of components were not given in the original publication. Therefore, the experimentally measured enthalpies of mixing of the liquid Au–Ag–Ge ternary alloys in Refs. [48,49] were employed only in the present optimization.

As for the phase relations of the Au–Ag–Ge ternary system, Hassam et al. [39] determined the three vertical sections: $Ag_{0.25}Au_{0.75}$–Ge, $Ag_{0.50}Au_{0.50}$–Ge and $Ag_{0.75}Au_{0.25}$–Ge using differential thermal analysis. Based on these experimental results, the liquidus projection of this ternary system was established. The experimental information [39] was taken into account in the present optimization.

3. Thermodynamic models

3.1. Pure elements

The stable forms of the pure elements at 298.15 K and 1 bar are chosen as the reference states. The Gibbs energy for the pure element i in ϕ status is given as:

$$ {}^{0}G_i^{\phi}(T) = G_i^{\phi}(T) - H_i^{SER} = a + b\cdot T + c\cdot T\ \ln T + d\cdot T^2 + e\cdot T^3 + f\cdot T^{-1} + g\cdot T^7 + h\cdot T^{-9} \quad (1) $$

where H_i^{SER} is the enthalpy of the element i in its standard reference state (SER) at 298.15 K and 1 bar; T is the absolute temperature in K; $G_i^{\phi}(T)$ is the Gibbs energy of the element i with structure ϕ; ${}^{0}G_i^{\phi}(T)$ is the molar Gibbs energy of the element i with the structure of ϕ referred to the enthalpy of its stable state at 298.15 K and 1 bar. In the present work, the Gibbs energies of the elements Au, Ag and Ge, ${}^{0}G_{Au}^{\phi}(T)$, ${}^{0}G_{Ag}^{\phi}(T)$ and ${}^{0}G_{Ge}^{\phi}(T)$ are taken from the SGTE (Scientific Group Thermodata Europe) database [33].

3.2. Solution phases

The substitutional solution model is employed to describe the solution phases including liquid, fcc_A1(Au,Ag), and diamond_A4(Ge), respectively. The molar Gibbs energy of the solution phase ϕ (ϕ = liquid, fcc_A1, and diamond_A4) can be expressed as:

$$ G_m^{\phi} = \sum x_i\, {}^{0}G_i^{\phi} + RT\sum x_i\ \ln(x_i) + {}^{E}G_m^{\phi} \quad (2) $$

where ${}^{0}G_i^{\phi}$ is the molar Gibbs energy of the element i (i = Ag, Au, Ge) with the structure ϕ, x_i the mole fraction of component i, R gas constant, T temperature in K, ${}^{E}G_m^{\phi}$ the excess Gibbs energy. The excess Gibbs energy of phase ϕ can be expressed with

Table 2
Thermodynamic parameters for the Au–Ag–Ge ternary system.

Phase	Thermodynamic parameter*	Reference
Liquid (Ag, Au, Ge)	${}^{(0)}L_{Ag,Au} = -16042 + 1.14T$	[30]
	${}^{(0)}L_{Ag,Ge} = +7636.87 - 6.822T$	
	${}^{(1)}L_{Ag,Ge} = -14500.14 + 5.761T$	This work
	${}^{(2)}L_{Ag,Ge} = -7029.56$	
	${}^{(0)}L_{Au,Ge} = -18294.684 - 13.671T$	
	${}^{(1)}L_{Au,Ge} = -8894.639 - 6.339T$	[16]
	${}^{(2)}L_{Au,Ge} = -2174.476 - 4.925T$	
	${}^{(0)}L_{Ag,Au,Ge} = -40000 + 5T$	
	${}^{(1)}L_{Ag,Au,Ge} = -110000 + 35T$	This work
	${}^{(2)}L_{Ag,Au,Ge} = +35000 + 5T$	
fcc_A1 (Ag,Au,Ge)	${}^{(0)}L_{Ag,Au} = -15599$	[30]
	${}^{(0)}L_{Ag,Ge} = +5696.47 + 9.917T$	This work
	${}^{(1)}L_{Ag,Ge} = -20237.27$	
	${}^{(0)}L_{Au,Ge} = +10198.859 - 23.114T$	[16]
diamond_A4 (Ge)	${}^{0}G_{Ge}^{dia.}$ cited from SGTE database	[33]

* *Note*: Gibbs energies are expressed in J/mol. The lattice stabilities of the elements Au, Ag and Ge in liquid, fcc_A1 and diamond_A4 were given by Dinsdale [33].

Redlich–Kister–Muggianu expression [54,55]:

$$ {}^{E}G_m^{\phi} = x_{Ag}x_{Au}\sum_{j=0}^{n} {}^{(j)}L_{Ag,Au}^{\phi}(x_{Ag}-x_{Au})^j + x_{Ag}x_{Ge}\sum_{j=0}^{n} {}^{(j)}L_{Ag,Ge}^{\phi}(x_{Ag}-x_{Ge})^j + x_{Au}x_{Ge}\sum_{j=0}^{n} {}^{(j)}L_{Au,Ge}^{\phi}(x_{Au}-x_{Ge})^j + x_{Ag}x_{Au}x_{Ge}L_{Ag,Au,Ge}^{\phi} \quad (3) $$

with

$$ {}^{(j)}L_{Ag,Ge}^{\phi} = A_j + B_jT \quad (4) $$

$$ L_{Ag,Au,Ge}^{\phi} = x_{Ag}\,{}^{(0)}L_{Ag,Au,Ge} + x_{Au}\,{}^{(1)}L_{Ag,Au,Ge} + x_{Ge}\,{}^{(2)}L_{Ag,Au,Ge} \quad (5) $$

where A_j and B_j are parameters to be optimized in the present work. ${}^{(j)}L_{Ag,Au}^{\phi}$ and ${}^{(j)}L_{Au,Ge}^{\phi}$ are binary interaction parameters, which are taken directly from the Au–Ag and Au–Ge binary systems assessed by Hassam et al. [30] and Wang et al. [16], respectively. The ternary interactive parameters ${}^{(j)}L_{Ag,Au,Ge}$ are parameters to be optimized in the present work.

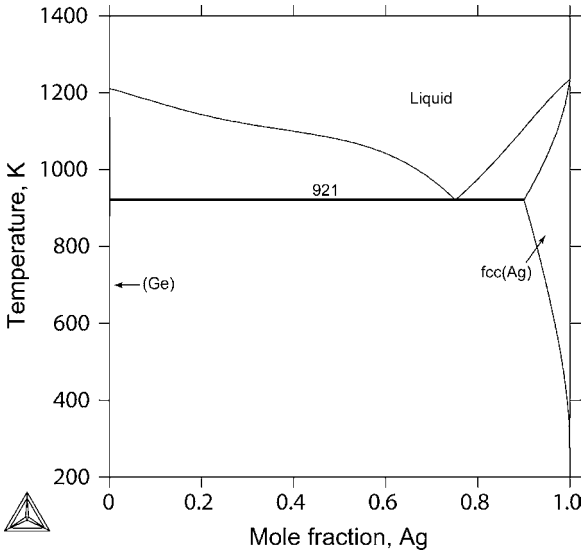

Fig. 3. Calculated phase diagram of the Ag–Ge binary system in the present work.

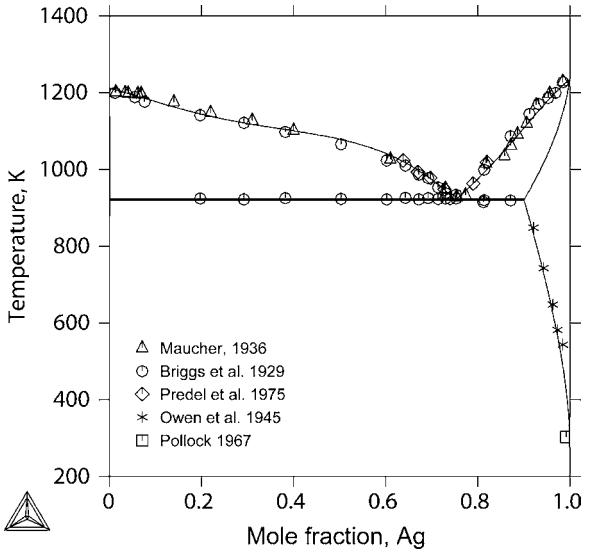

Fig. 4. Comparison of the calculated phase diagram of the Ag–Ge binary system with experimental data [35,36,38,40,41] in the present work.

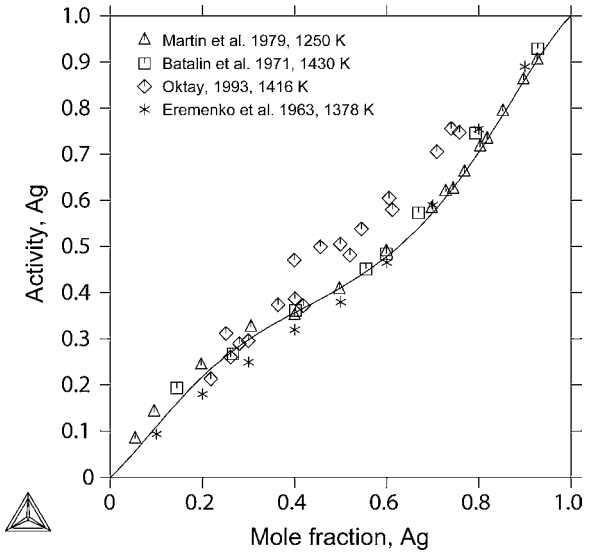

Fig. 6. Calculated activity of Ag with the experimental data [44–47] at 1250 K (Ref. state: liquid Ag).

4. Results and discussion

Using the lattice stabilities of the elements Au, Ag and Ge compiled by Dinsdale [33], the model parameters for various phases in the Au–Ag–Ge ternary system was optimized using the PARROT module in the Thermo-calc® software package developed by Sundman et al. [34]. This module works by minimizing the square sum of the differences between experimental data and calculated values. In the optimization procedure, each set of experimental data is given a certain weight according to the reliability and compatibility of experimental data. It should be claimed that the weights of much more reliable experimental data are larger than those of less ones during the optimization. For thermodynamic data, in general, the activity of a component determined by the EMF method are much more reliable and within a smaller experimental error than that determined by vapour pressure method, while the enthalpies of mixing of liquid alloys obtained directly by calorimetry are much more believable than that derived from indirect measurements (such as EMF). As for phase diagram data, it is better to use the measured experimental data by thermal analysis method. The weights can be changed systematically during the optimization until most of experimental data is accounted for within the claimed uncertainty limits. Thermodynamic parameters for all condensed phases in the Au–Ag–Ge ternary system used and obtained finally in the present work are summarized in Table 2.

4.1. The Ag–Ge binary system

Fig. 3 shows the calculated phase diagram of the Ag–Ge binary system. The comparison of the calculated phase diagram with the experimental data by Briggs et al. [35], Maucher [36], Hume-Rothery et al. [37], Predel and Bamlstahl [38], Hassam et al. [39], Owen and Rowlands [40] and Pollock [41] is presented in Fig. 4. The calculated liquidus is in agreement with the experimental data [35,36,38]. The calculated temperature and composition of the eutectic reaction agree well with the experimental data [35–39] and the previously assessed values [32] as given in Table 1. Therefore, the reasonable agreement is obtained between the calculated

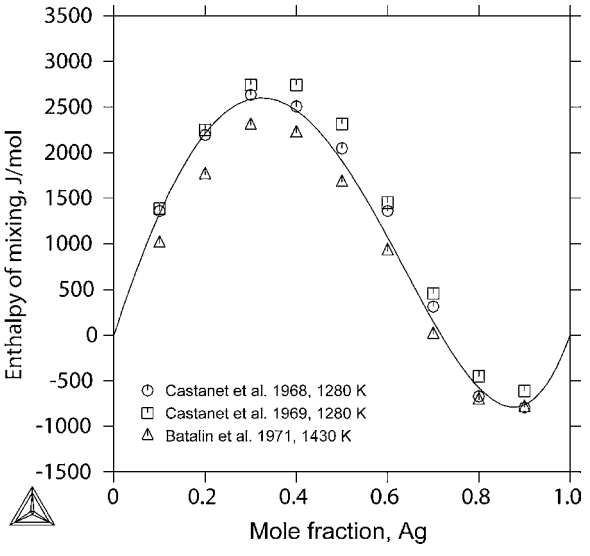

Fig. 5. Calculated enthalpies of mixing of liquid Ag–Ge alloys at 1250 K in comparison with the experimental data [42–44] (Ref. states: liquid Ag and Ge).

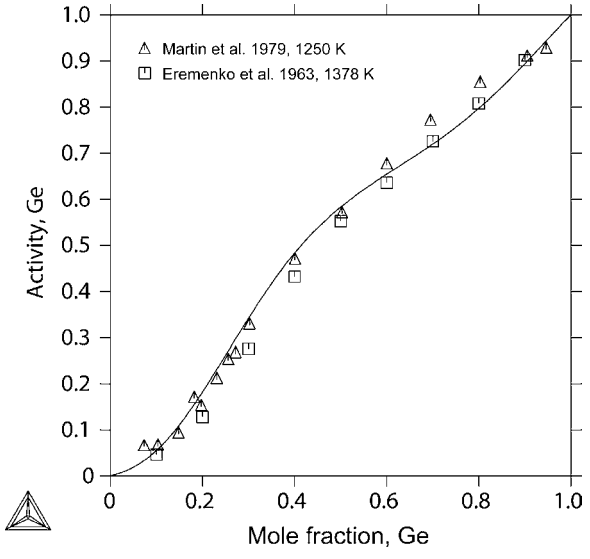

Fig. 7. Calculated activity of Ge with the experimental data [45,46] at 1250 K (Ref. state: liquid Ge).

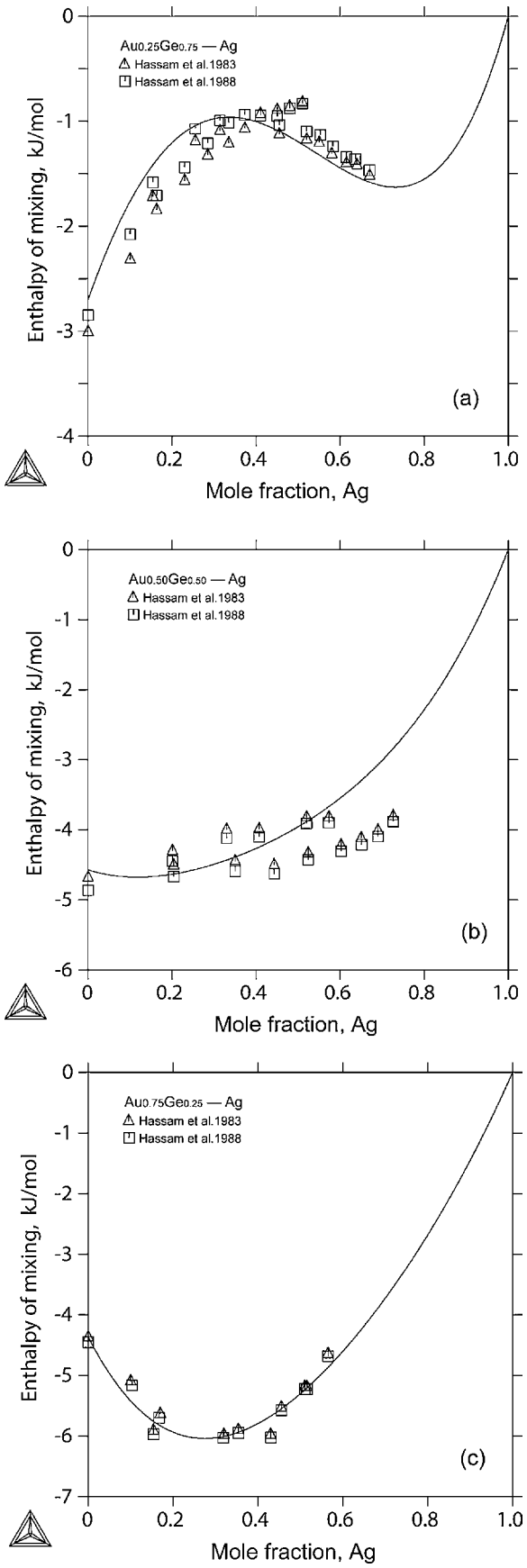

Fig. 8. Comparison of the calculated enthalpies of mixing of liquid Au–Ag–Ge ternary alloys with the experimental data [48,49] referred to liquid Ag, Au and Ge at 1373 K. (a) $Au_{0.25}Ge_{0.75}$–Ag; (b) $Au_{0.50}Ge_{0.50}$–Ag and (c) $Au_{0.75}Ge_{0.25}$–Ag.

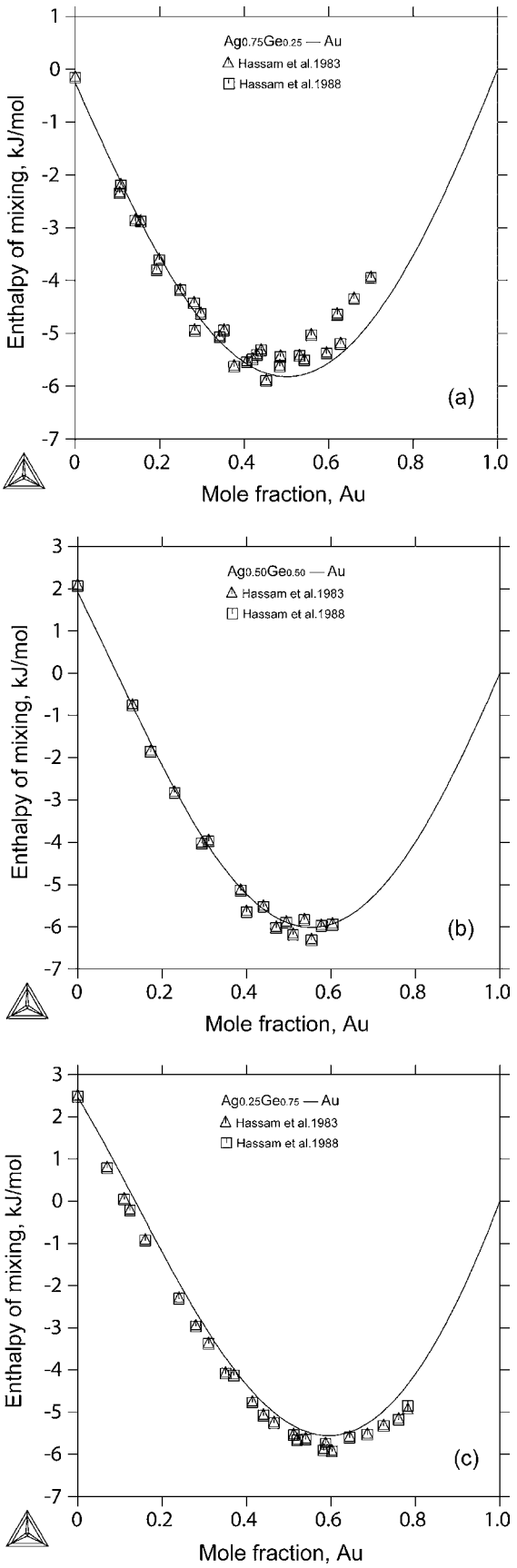

Fig. 9. Comparison of the calculated enthalpies of mixing of liquid Au–Ag–Ge ternary alloys with the experimental data [48,49] referred to liquid Ag, Au and Ge at 1373 K. (a) $Ag_{0.75}Ge_{0.25}$–Au; (b) $Ag_{0.50}Ge_{0.50}$–Au and (c) $Ag_{0.25}Ge_{0.75}$–Au.

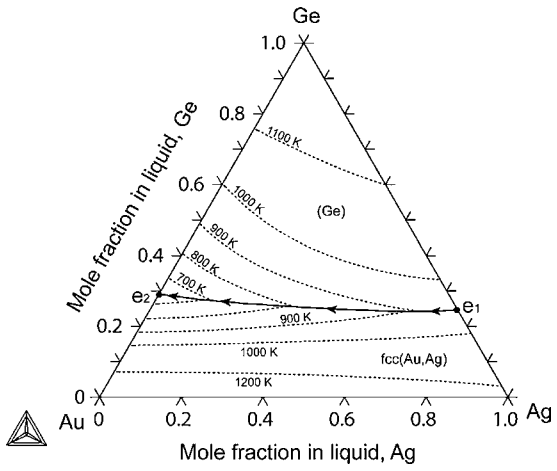

Fig. 10. Calculated liquidus projection of the Au–Ag–Ge ternary system in the present work.

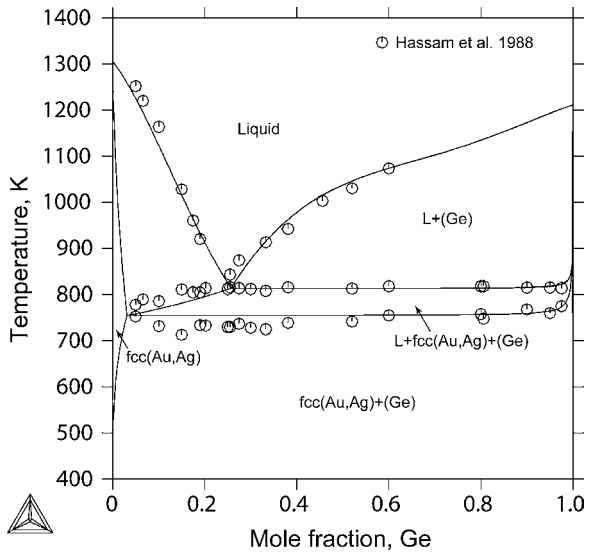

Fig. 12. Calculated vertical section of $Ag_{0.50}Au_{0.50}$–Ge with the experimental data [39].

results and the experimental information [35–39] in the present work.

The comparison of the enthalpies of mixing of the liquid Ag–Ge alloys between the calculated and experimental values at 1280 K is shown in Fig. 5. It can be seen that the calculated mixing enthalpies agree with the experimental data by Castanet et al. [42,43] and Batalin et al. [44] if considering the experimental error.

Fig. 6 compares the calculated activity of Ag in liquid Ag–Ge alloys at 1250 K with the experimental data determined by Batalin et al. [44], Eremenko et al. [45], Martin-Garin et al. [46] and Oktay [47]. The calculated activity of Ag is reasonably consistent with the experimental data [44–46], but shows an obvious deviation with the experimental data [47]. Fig. 7 shows the comparison of the calculated activity of Ge in liquid Ag–Ge alloys at 1250 K with the experimental data measured by Eremenko et al. [45] and Martin-Garin et al. [46]. The calculated activity of Ge is in good agreement with the experimental data [45,46].

4.2. The Au–Ag–Ge ternary system

Combining the present optimization of the Ag–Ge binary system with the previous assessments of the Au–Ag and Au–Ge binary systems, the Au–Ag–Ge ternary system has been further optimized based on available experimental data. Thermodynamic properties of liquid alloys, liquidus projection and several vertical sections of this ternary system are also calculated and compared with the experimental data in Figs. 8–13. Reasonable agreements are achieved between the calculated results and the experimental data.

Enthalpies of mixing of the liquid Au–Ag–Ge ternary alloys at 1373 K along different across sections were calculated in comparisons with the experimental data measured by Hassam and Gaune-Escard [48] and Hassam et al. [49] as shown in Figs. 8 and 9. As can be seen, the calculated enthalpies of mixing of the liquid ternary alloys along two cross-sections with Ag to Ge ratio of 1:3 and 1:1 at 1373 K show slight deviation from the experimental data [48,49] in Fig. 8(a) and (b). However, the good agreements are achieved between the calculated enthalpies of mixing of the liquid Au–Ag–Ge ternary alloys along three cross sections with Ag to Ge ratio of 3:1, 1:1 and 1:3 and the experimental data at 1373 K in Fig. 9. The calculated results in the present work are still reasonable and acceptable if one considers the experimental error (about

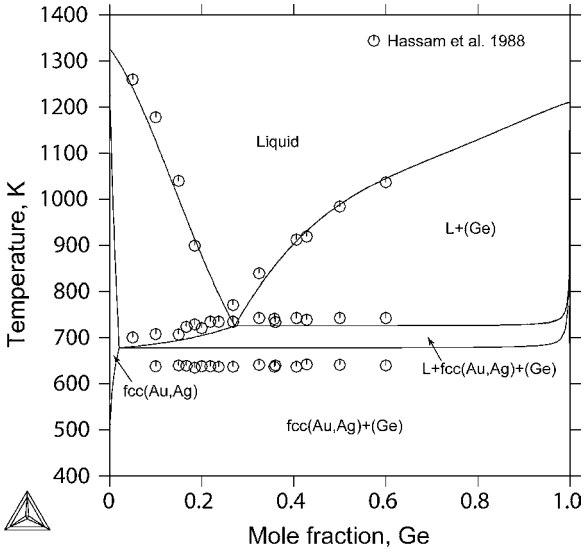

Fig. 11. Calculated vertical section of $Ag_{0.25}Au_{0.75}$–Ge with the experimental data [39].

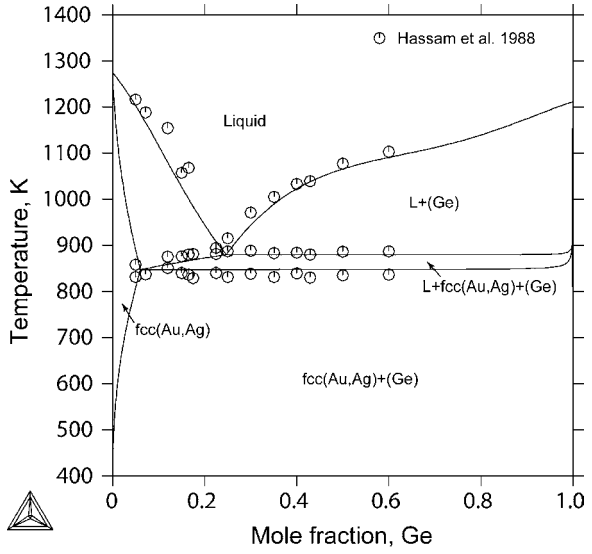

Fig. 13. Calculated vertical section of $Ag_{0.75}Au_{0.25}$–Ge with the experimental data [39].

8%) of the data measured by Hassam and Gaune-Escard [48] and Hassam et al. [49].

In the Au–Ag–Ge ternary system, invariant reaction associated with liquid phase is a ternary monovariant eutectic reaction. Fig. 10 is the calculated liquidus projection of this ternary system. The monovariant curve e_1e_2 runs smoothly from the Ag–Ge binary eutectic point e_1 to the Au–Ge binary eutectic point e_2.

Figs. 11–13 are the calculated vertical sections of $Ag_{0.25}Au_{0.75}$–Ge, $Ag_{0.50}Au_{0.50}$–Ge and $Ag_{0.75}Au_{0.25}$–Ge in the Au–Ag–Ge ternary system with the experimental data [39], respectively. As can be seen, the calculated phase relations and phase boundaries in Figs. 12 and 13 are in good agreement with the experimental data [39]. In Fig. 11, the calculated phase relations of the $Ag_{0.25}Au_{0.75}$–Ge section are consistent with the experimental results, although the calculated phase boundary for the three-phase field, L + fcc(Au,Ag) + (Ge), shows a slight deviation from the experimental data measured by Hassam et al. [39].

5. Conclusions

The Ag–Ge binary system has been reassessed using the CALPHAD method through Thermo-calc® software package. A set of self-consistent parameters for describing various phases in the Ag–Ge binary system was obtained, which can be used to reproduce well the reported experimental data including phase diagram and thermodynamic properties. Combined the previous assessments of the Au–Ag and Au–Ge binary systems with the available experimental information on the Au–Ag–Ge ternary system, the thermodynamic description of the Au–Ag–Ge ternary system has been developed. The liquidus projection and several vertical sections were calculated. The calculated results are in good agreement with the reported experimental data.

Acknowledgements

This work was financially supported by Scientific Research Foundation for Advanced Talents in Guilin University of Electronic Technology, National Science Foundation of China (Grant Nos. 50771106, 50971136 and 50731002) and Key Project of Chinese Ministry of Education (No. 109122).

References

[1] T. Braun, K.F. Becker, M. Koch, V. Bader, Microelectron. Reliab. 46 (2006) 144–154.
[2] V. Chidambaram, J. Hald, R. Ambat, J. Hattel, JOM 61 (6) (2009) 59–65.
[3] K. Suganuma, S.-J. Kim, K.-S. Kim, JOM 61 (1) (2009) 64–71.
[4] J.Y. Tsai, C.W. Chang, Y.C. Shieh, Y.C. Hu, C.R. Kao, J. Electron. Mater. 34 (2005) 182–187.
[5] Q. Wang, S.-H. Choa, W. Kim, J. Hwang, S. Ham, C. Moon, J. Electron. Mater. 35 (2006) 425–432.
[6] J.S. Kim, W.S. Choi, D. Kim, A. Shkel, C. Lee, Mater. Sci. Eng. A 458 (2007) 101–107.
[7] J.-W. Yoon, H.-S. Chun, S.-B. Jun, Mater. Sci. Eng. A 473 (2008) 119–125.
[8] G.S. Zhang, H.Y. Jing, L.Y. Xu, J. Wei, Y.D. Han, J. Alloys Compd. 476 (2009) 138–141.
[9] D.Q. Yu, H. Oppermann, J. Kleff, M. Hutter, J. Mater. Sci. Mater. Electron. 20 (2009) 55–59.
[10] V. Chidambaram, J. Hald, J. Hattel, Microelectron. Reliab. 49 (2009) 323–330.
[11] V. Chidambaram, J. Hald, J. Hattel, J. Alloys Compd. 490 (2010) 170–179.
[12] J. Wang, H.S. Liu, Z.P. Jin, CALPHAD 28 (2004) 91–95.
[13] J. Wang, H.S. Liu, L.B. Liu, Z.P. Jin, Trans. Nonferrous Met. Soc. China 17 (2007) 1405–1411.
[14] J. Wang, H.S. Liu, L.B. Liu, Z.P. Jin, CALPHAD 31 (2007) 545–552.
[15] J. Wang, F.G. Meng, H.S. Liu, L.B. Liu, Z.P. Jin, J. Electron. Mater. 36 (2007) 568–577.
[16] J. Wang, C. Leinenbach, M. Roth, J. Alloys Compd. 481 (2009) 830–836.
[17] J. Wang, C. Leinenbach, M. Roth, J. Alloys Compd. 485 (2009) 577–582.
[18] J. Wang, C. Leinenbach, M. Roth, International Conference *CALPHAD XXXVIII*, Prague, Czech Republic, May 17–22, 2009.
[19] J. Wang, F.G. Meng, M.H. Rong, L.B. Liu, Z.P. Jin, Thermochim. Acta 505 (2010) 79–85.
[20] J. Wang, Y.J. Liu, L.B. Liu, H.Y. Zhou, Z.P. Jin, (2010) unpublished work.
[21] H.S. Liu, C.L. Liu, C. Wang, Z.P. Jin, K. Ishida, J. Electron. Mater. 32 (2003) 81–88.
[22] H.S. Liu, C.L. Liu, K. Ishida, Z.P. Jin, J. Electron. Mater. 32 (2003) 1290–1296.
[23] H.S. Liu, K. Ishida, Z.P. Jin, Y. Du, Intermetallics 11 (2003) 987–994.
[24] H.S. Liu, Y. Cui, K. Ishida, Z.P. Jin, CALPHAD 27 (2003) 27–37.
[25] H.S. Liu, J. Wang, Y. Du, Z.P. Jin, Z. Metallkd. 95 (2004) 45–49.
[26] F.G. Meng, H.S. Liu, L.B. Liu, Z.P. Jin, J. Alloys Compd. 431 (2007) 292–297.
[27] H.Q. Dong, S. Jin, L.G. Zhang, J.S. Wang, X.M. Tao, H.S. Liu, Z.P. Jin, J. Electron. Mater. 38 (2009) 2158–2169.
[28] L. Kaufman, H. Bernstein, Computer Calculation of Phase Diagrams, Academic Press, New York, America, 1970.
[29] N. Saunders, A.P. Modwnik, CALPHAD – A Comprehensive Guide, Pergamon, Lausanne, Switzerland, 1998.
[30] S. Hassam, J. Ågren, M. Gaune-Escard, J.P. Bros, Metall. Trans. A 21 (1990) 1877–1884.
[31] R.W. Olesinki, G.J. Abbaschian, Bull. Alloy Phase Diagrams 9 (1988) 58–64.
[32] P.-Y. Chevalier, Thermochim. Acta 130 (1988) 25–32.
[33] A.T. Dinsdale, CALPHAD 15 (1991) 317–425.
[34] B. Sundman, B. Jansson, J.-O. Andersson, CALPHAD 9 (1985) 153–190.
[35] T.R. Briggs, R.O. McDuffie, L.H. Willisford, J. Phys. Chem. 33 (1929) 1080–1096.
[36] H. Maucher, Forschungsarb. Metallkd. Röntgenmet. 20 (1936) 1–32.
[37] W. Hume-Rothery, G.V. Raynor, P.W. Reynolds, H.K. Packer, J. Inst. Met. 66 (1940) 209–239.
[38] B. Predel, H. Bamlstahl, J. Less-Common Met. 43 (1975) 191–203.
[39] S. Hassam, M. Gambino, M. Gaune-Escard, J.P. Bros, J. Ågren, Metall. Trans. A 19 (1988) 409–416.
[40] E.A. Owen, V.W. Rowlands, J. Inst. Met. 66 (1940) 361–379.
[41] D.D. Pollock, Trans. Metall. Soc. AIME 239 (1967) 1768–1770.
[42] R. Castanet, M. Laffitte, C.R. Hebd. Séances Acad. Sci. Ser. C 267 (1968) 204–206.
[43] R. Castanet, Y. Claire, M. Laffitte, J. Chim. Phys. 66 (1969) 1276–1285.
[44] G.I. Batalin, E.A. Beloborodova, V.A. Stukalo, Russ. J. Phys. Chem. 45 (1971) 1533.
[45] V.N. Eremenko, G.M. Lukashenko, V.L. Pritula, Izv. Akad. Nauk SSSR, Neorg. Mater. 3 (1967) 1584–1590.
[46] L. Martin-Garin, C. Chatillon, M. Allibert, J. Less-Common Met. 63 (1979) P9–P23.
[47] E. Oktay, Mater. Tech. 81 (1993) 101–106.
[48] S. Hassam, M. Gaune-Escard, High Temp. Sci. 16 (1983) 131–151.
[49] S. Hassam, M. Gaune-Escard, J.P. Bros, M. Hoch, Metall. Trans. A 19 (1988) 2075–2089.
[50] R. Castanet, J. Less-Common Met. 136 (1988) 287–296.
[51] Q. Yu, S.M. Howard, Mater. Res. Soc. Symp. Proc. 291 (1993) 425–430.
[52] A. Prince, G.V. Raynor, D.S. Evans, Phase Diagrams of Ternary Gold Alloys, The Institute of Metals, London, 1990.
[53] G. Borzone, S. Hassam, J.P. Bros, Metall. Trans. A 20 (1989) 2167–2170.
[54] O. Redlich, A.T. Kister, Ind. Eng. Chem. 40 (1948) 345–348.
[55] Y.M. Muggianu, M. Gambino, J.P. Bros, J. Chim. Phys. 72 (1975) 83–88.